

Supporting Information

Title: Ultrasmall Endogenous Biopolymer Nanoparticles for Magnetic Resonance/Photoacoustic Dual-Modal Imaging-Guided Photothermal Therapy

Jinghua Sun^a, Wen Xu^b, Liping Li^d, Bo Fan^d, Xiaoyang Peng^a, Botao Qu^d, Lingjie Wang^b, Tingting Li^a, Sijin Li^c and Ruiping Zhang^{*b}

^a Center for Translational Medicine Research, Shanxi Medical University, Taiyuan 030001, China

^b Imaging Department of Affiliated Tumor Hospital of Shanxi Medical University, Imaging Department of Shanxi Provincial Cancer Hospital; Imaging Department of Shanxi Medical University, Radiology Department of the First Hospital of Shanxi Medical University, Taiyuan 030001, China

^c Nuclear Medicine Department of the First Hospital of Shanxi Medical University, Taiyuan 030001, China

^d Shanxi Medical University, Taiyuan 030001, China

*E-mail: zrp_7142@163.com.

Jinghua Sun and Wen Xu contributed equally to this work.

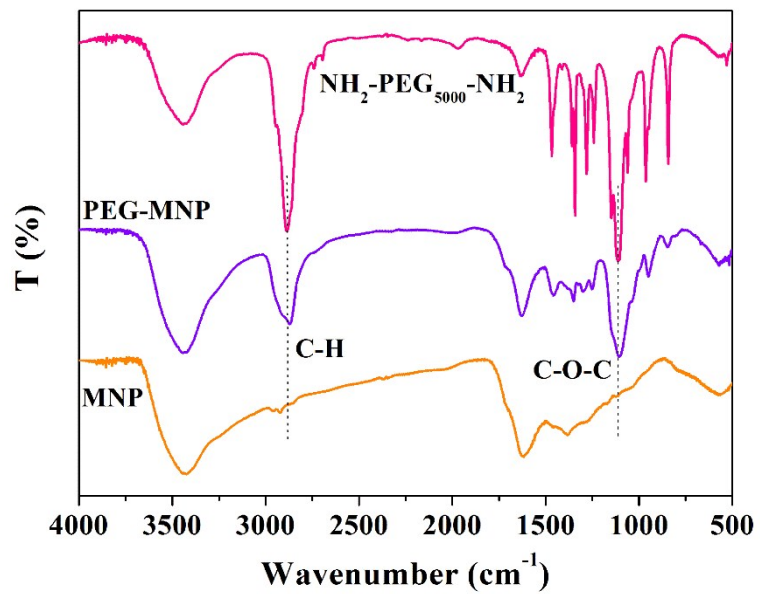


Fig. S1 FT-IR spectra of MNP, PEG-MNP and $\text{NH}_2\text{-PEG}_{5000}\text{-NH}_2$.

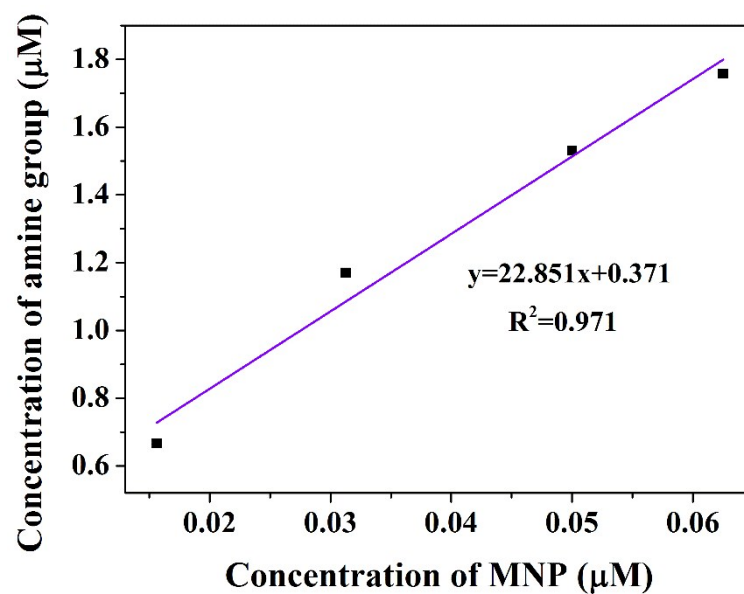


Fig. S2 Relationship of MNP-PEG with the amine group determined by fluorescamine.

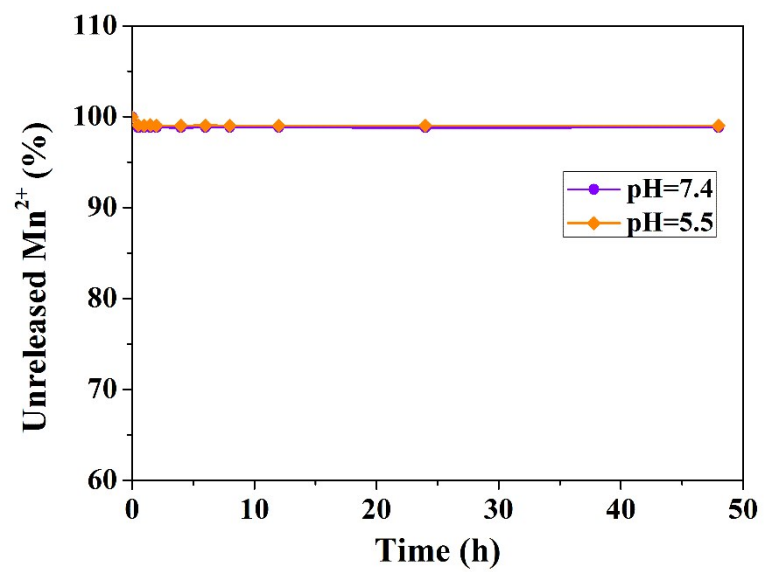


Fig. S3 Mn²⁺ stability study of MNP-Mn in PBS (pH=7.4) and acidic buffer solution (pH=5.5).

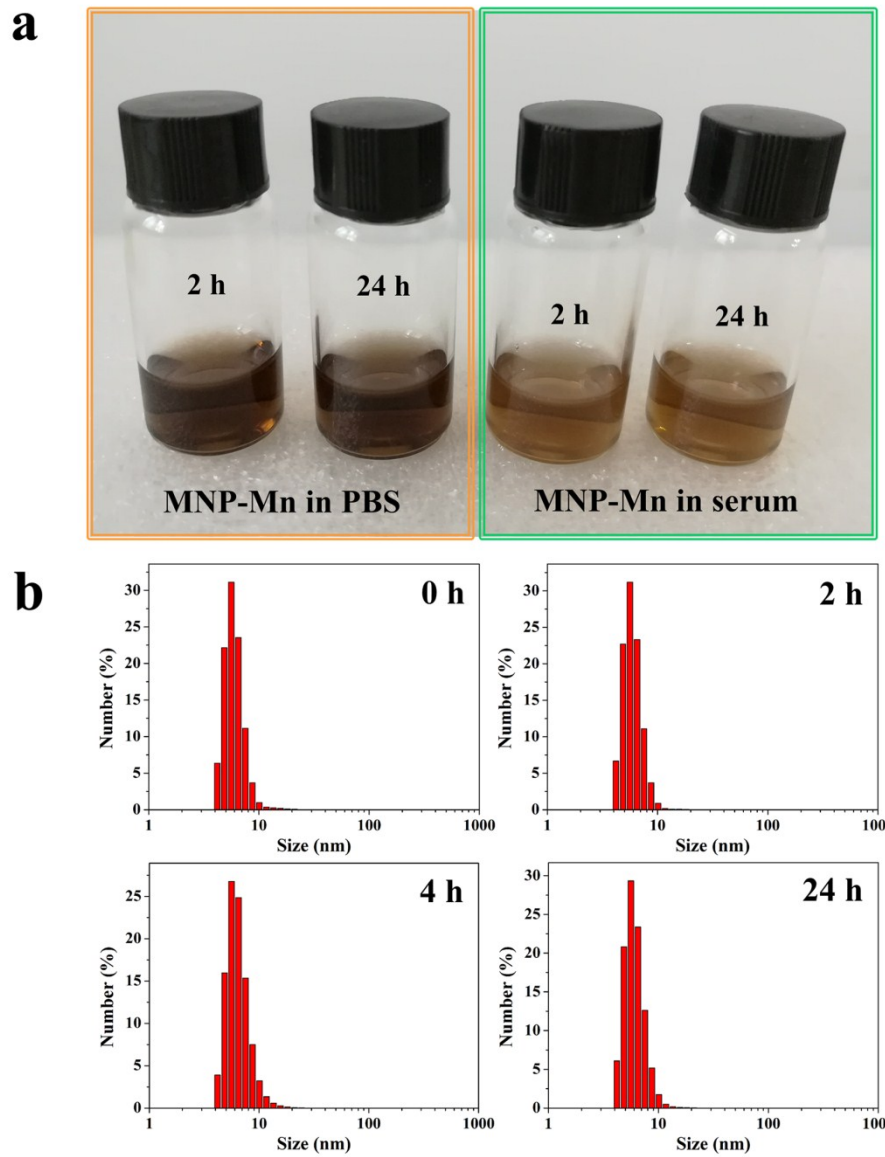


Fig. S4 (a) photos of MNP-Mn in PBS and serum with different incubation time. (b) Hydrodynamic size distribution of the MNP-Mn during different incubation periods with serum, suggesting good stability in serum.

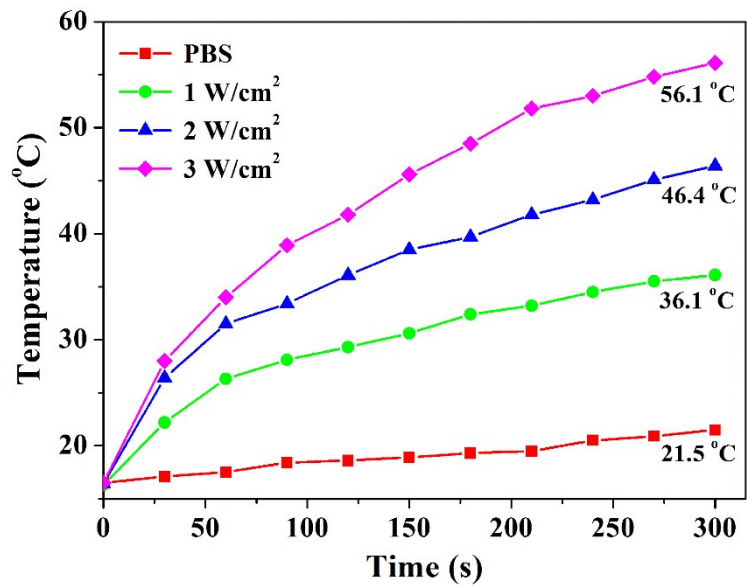


Fig. S5 Temperature curves of MNP-Mn with the same concentration (200 $\mu\text{g/mL}$) and PBS irradiated by an 808 nm laser at different laser power density for 5 min.

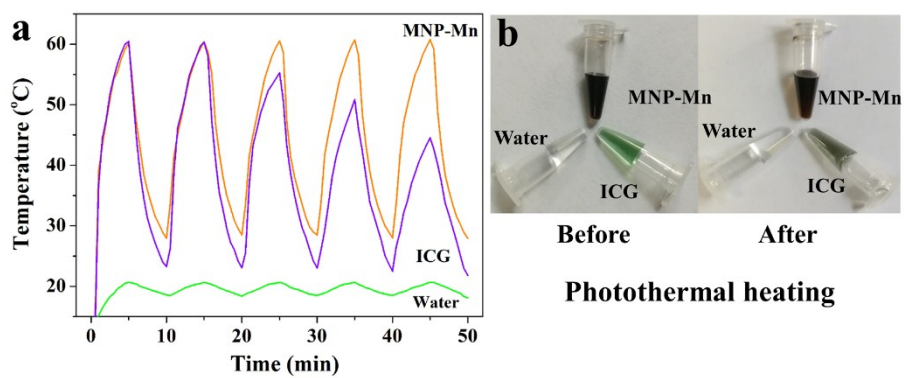


Fig. S6 (a) Temperature curves of MNP-Mn, ICG solutions and water under five cycles of photothermal heating by an 808 nm laser. (b) Photos of MNP-Mn, ICG solutions and water before and after photothermal heating.

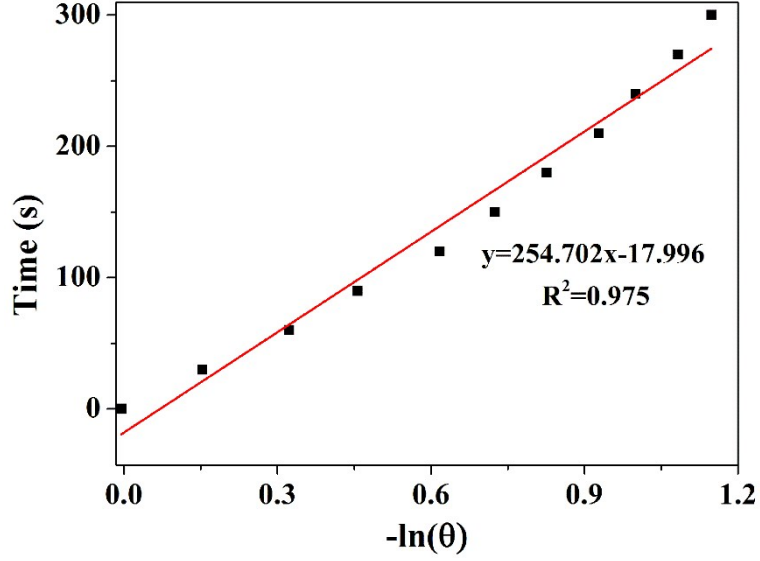


Fig. S7 Linear time data versus $-\ln(\theta)$ obtained from the cooling period.

The photothermal conversion efficiency of the MNP-Mn was calculated as following:

$$\eta = \frac{hs(T_{Max} - T_{Surr}) - Q_{Dis}}{I(1 - 10^{-A_{808}})} \quad (1)$$

The photothermal conversion efficiency η can be obtained from Eq.1. Where h is the heat transfer coefficient, s is the surface area of the container. The maximum steady temperature (T_{Max}) of the MNP-Mn solution was 60.2 °C and environmental temperature (T_{Surr}) was 13.2 °C. So, the temperature change ($T_{Max} - T_{Surr}$) of the MNP-Mn solution was 47 °C. The laser power I is 0.6 W. The absorbance of the MNP-Mn at 808 nm A_{808} is 0.732. Q_{Dis} expresses heat dissipated from the light absorbed by the solvent and container. The value of hs is obtained from the Eq.2, where τ_s can be obtained from Eq.3.

$$hs = \frac{mDC_D}{\tau_s} \quad (2)$$

$$t = -\tau_s \ln\left(\frac{T - T_{Surr}}{T_{Max} - T_{Surr}}\right) \quad (3)$$

According to Figure S7, τ_s was determined and calculated to be 254.72 s. In addition, m is 0.13 g and C is 4.2 J/g°C. Thus, according to Eq. 2, hs is deduced to be 2.11 mW/°C. Q_{Dis} was measured independently to be 9.35 mW. Thus, substituting

according values of each parameters to Eq.1, the 808 nm laser heat conversion efficiency of the MNP-Mn can be calculated to be 18.4 %.

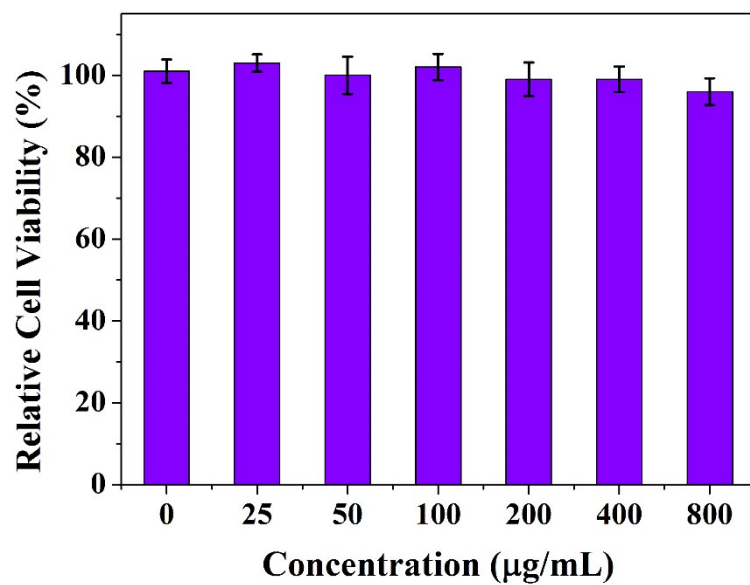


Fig. S8 Cell viabilities of the NIH 3T3 cells after 24 h incubation with MNP-Mn at various concentrations by MTT assay.

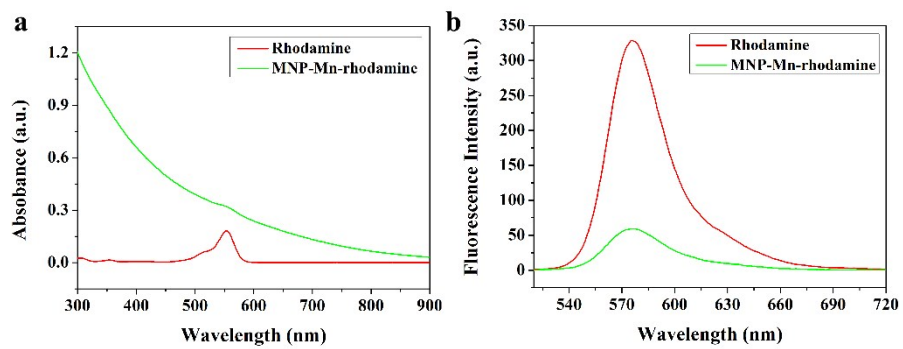


Fig. S9 UV-Vis and fluorescence spectra of rhodamine and MNP-Mn-rhodamine solutions.

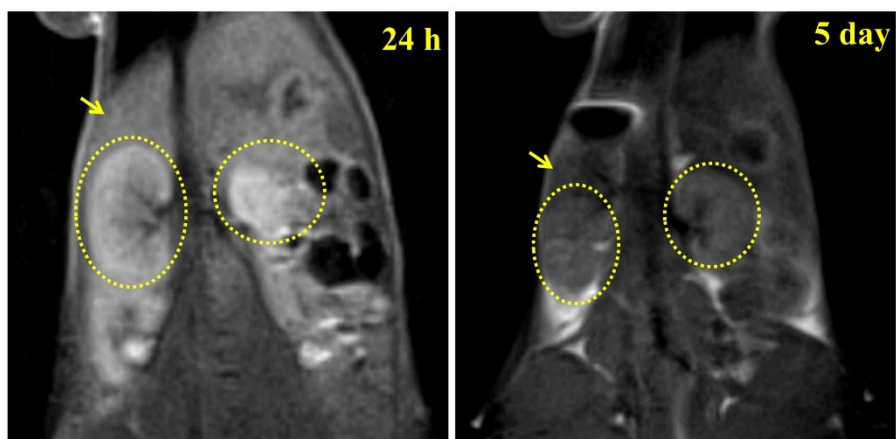


Fig. S10 T_1 -weighted MR coronal images after i.t. injection into the tumor bearing mice at 24 h and 5 day using 3.0 T clinical MRI equipment. The livers and kidneys are highlighted by yellow arrows and circles, respectively.